porousMedia4Foam: Multi-scale open-source platform for hydro-geochemical simulations with OpenFOAM®

Cyprien Soulaine, Saideep Pavuluri, Francis Claret, Christophe Tournassat

Journal Pre-proof

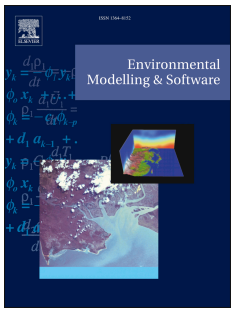

porousMedia4Foam: Multi-scale open-source platform for hydro-geochemical simulations with OpenFOAM®

Cyprien Soulaine, Saideep Pavuluri, Francis Claret, Christophe Tournassat

PII: S1364-8152(21)00241-3

DOI: https://doi.org/10.1016/j.envsoft.2021.105199

Reference: ENSO 105199

To appear in: *Environmental Modelling and Software*

Accepted Date: 7 September 2021

Please cite this article as: Soulaine, C., Pavuluri, S., Claret, F., Tournassat, C., *porousMedia4Foam*: Multi-scale open-source platform for hydro-geochemical simulations with OpenFOAM®, *Environmental Modelling and Software*, https://doi.org/10.1016/j.envsoft.2021.105199.

porousMedia4Foam: Multi-scale open-source platform for hydro-geochemical simulations with OpenFOAM®

Cyprien Soulaine[a], Saideep Pavuluri[c,a], Francis Claret[c], Christophe Tournassat[b,d]

[a] *Earth Sciences Institute of Orlans, CNRS-Universit d'Orlans-BRGM, Orlans, France*
[b] *Univ. Orlans, CNRS, BRGM, ISTO, UMR 7327, F-45071, Orlans, France*
[c] *BRGM, French Geological Survey, Orlans, France*
[d] *Energy Geosciences Division, Lawrence Berkeley National Laboratory, Berkeley, CA, USA*

Abstract

porousMedia4Foam is a package for solving flow and transport in porous media using OpenFOAM® - a popular open-source numerical toolbox. We introduce and highlight the features of a new generation open-source hydro-geochemical module implemented within *porousMedia4Foam*, which relies on micro-continuum concept and which makes it possible to investigate hydro-geochemical processes occurring at multiple scales i.e. at the pore-scale, reservoir-scale and at the hybrid-scale. Geochemistry is handled by a third party package (e.g. PHREEQC) that is coupled to the flow and transport solver of OpenFOAM®. We conducted benchmarks across different scales to validate the accuracy of our simulator. We further looked at the evolution of mineral dissolution/ precipitation in a fractured porous system. Application fields of this new package include the investigation of hydro-bio-geochemical processes in the critical zone, the modelling of contaminant transport in aquifers, as well as and the assessment of confinement performance for geological barriers.

Keywords: Reactive Transport Modelling, Multi-scale simulations, Micro-continuum, OpenFOAM, PHREEQC

1. Introduction

Over the last decades, reactive transport modelling (RTM) has become an essential tool for the study of subsurface processes involving flow, transport and geochemical reactions [1]. This discipline is at the junction of two scientific communities, namely geochemistry and transport in porous media. RTM consists of computational models that describe the coupled physical, chemical, and biological processes that interact with each other over a broad range of spatial and temporal scales. RTM modelling tools enable the prediction of contaminant migration in polluted aquifers, and are used to design enhanced remediation techniques. Integration of physical and biogeochemical processes makes RTM also an ideal research instrument for elucidating the complex and non-linear interactions between roots, micro-organisms, water composition and minerals in the Critical Zone [2]. Other applications include the assessment of the long-term integrity of reservoirs for storing carbon dioxide, hydrogen or nuclear wastes in deep geological formations [3, 4]. In practice, three different

kinds of models are used to describe reactive transport in porous media as illustrated in Figure 1: *(i)* continuum models, *(ii)* pore-scale models, and *(iii)* hybrid models that combine both former approaches.

Continuum models (see Fig. 1c) are representative of the historical and standard approach for solving reactive transport in large-scale natural porous systems [5]. Continuum-scale RTM codes include, among others, MIN3P [6], CrunchFlow [1], TOUGHREACT [7], PFlotran [8] or HP1 [9]. In such codes, flow and transport equations are formulated in terms of volume-averaged equations with respect to a Representative Elementary Volume (REV) of the porous structure [10] and are coupled with geochemical reactions (see Steefel et al. [1] for an comprehensive description of the coupling). The topology of the rock micro-structures is described using effective properties including porosity, tortuosity, permeability – or hydraulic conductivity – and specific surface area. Flow is usually modelled using Darcy's law and multi-component species transport relies on a set of advection-dispersion-reaction equations. In addition to the classic challenges related to transport in porous media, including the medium heterogeneity awareness and the description of hydrodynamic dispersion, RTM has to consider the variation of rock properties in response to chemical reactions. Indeed, by enlarging or clogging pore throats and fractures, geochemical processes such as minerals dissolution and precipitation can alter the local flowfield and subsequently modify the rock properties, e.g permeability, tortuosity, accessible reactive surface area [11, 12].

Changes in rock properties with chemical reaction is usually described in continuum-scale RTM as heuristic functions of the porosity. For example, in most of reactive transport codes, tortuosity is described using Archies's law, permeability change is modelled using Kozeny-Carman relationship, and mineral surface areas evolve as a two-third power law of the porosity [13]. However, the complex interplay between reactions, advection, and diffusion can lead to highly nonlinear porosity feedback that is poorly captured using this kind of relationships that were not built on a strong theoretical background [14, 15]. The limiting factor of the continuum-scale models is therefore the determination of empirical parameters and their evolution as a function of the progress of geochemical processes. To circumvent these challenges, recent efforts have focused on the numerical modelling of coupled hydro-geochemical processes at the pore-scale [16, 17, 18, 19, 20].

In pore-scale models (see Fig. 1a), the pore network is fully resolved, i.e. each point of space is occupied by either a fluid or solid phase. As the exact knowledge of the phase distribution is known, continuum-scale concepts such as porosity, permeability, and reactive surface area do not apply at the pore-scale. They can be obtained, however, by averaging pore-scale simulation results if the computational domain is large enough to reach the size of a REV [21, 22]. The strategy that consists in simulating flow and transport in a three-dimensional image of a porous sample to characterize its continuum-scale properties has become an independent scientific discipline sometimes referred to as Digital Rock Physics [23, 24, 25, 26]. Most of the efforts so far have been devoted to solve the Navier-Stokes equations under single [27, 28, 29, 30] and two-phase flow conditions [31, 32, 33, 34, 35] to compute absolute and relative permeabilities. Despite the growing investment in the development of RTM at the pore-scale – pioneer simulators date back to the late 90s [16] – the

pore-scale RTM field is still emerging. One of the main challenge of this approach consists in moving the fluid/solid boundary with respect to chemical reactions at the mineral boundaries [36]. A comprehensive review of the different approaches used to solve this problem can be found in Molins et al. [37]. It is only very recently that pore-scale simulators have been proved mature for reproducing accurately and without any adjusting parameters the dissolution of a calcite crystal [38, 37], or of a gypsum grain [39]. Actually, the benchmark presented in Molins et al. [37] is a first effort based on a relatively simple geochemical reaction (a single component that reacts with a single mineral using a first-order kinetics) to demonstrate the ability of current codes to accurately simulate mineral dissolution at the pore scale in a reproducible manner with several codes. Further developments and verifications still need to be done for simulating multi-component aqueous solutions interacting with heterogeneous multi-mineral media using comprehensive reaction networks.

Naturally occurring porous media involve a wide range of spatial scales. For example, the important contrast in pore-size distributions in fractured porous rocks comes from much larger characteristic lengths for the fractures than for the surrounding porous matrix. Therefore, the domain size required to reach a REV limits the use of pure pore-scale modelling. Hybrid-scale models have been proposed to describe systems that include multiple characteristic length-scales, for which some regions are described using pore-scale modelling while others are modelled with continuum approaches (see Fig. 1b) [40, 41]. Two different approaches have been developed to solve hybrid-scale problems. On the one hand, the domain decomposition technique solves different physics on separate domains – one for Darcy flow, another for Stokes flow – linked together through appropriate boundary conditions [42] including Beaver-Joseph and Ochoa-Tapia-Whitaker conditions [43, 44]. On the other hand, micro-continuum models use a single set of partial differential equations throughout the computational domain regardless of the content of a grid block [45, 46]. The latter approach is particularly well-suited to capture the dynamic displacement of the interface between the porous and solid-free regions without involving complex re-meshing strategies. For example, micro-continuum models have been used successfully to simulate the formation and growth of wormholes in acidic environments [47, 48, 46]. Hybrid-scale modelling is also a powerful tool in image-based simulations to account for microscale features that are not visible in the images because they are smaller than the imaging instrument resolution [49, 50, 51, 30, 52].

In this study, we developed a comprehensive open-source simulator to model coupled hydro-geochemical processes at continuum-, pore- and hybrid-scales. This unique multi-scale framework relies on the micro-continuum model and its ability to tend asymptotically toward continuum-scale models if grid block contains solid content ($0 < \phi < 1$) or towards pore-scale models otherwise ($\phi = 1$) [46]. The resulting advanced RTM allows the treatment of complex reactions network as a function of flow conditions, water composition and minerals distribution within the rock including the complex porosity feedback between flow and chemistry. It is part of *porousMedia4Foam*, an open-source package developed by the authors to solve flow and transport in porous media within the popular simulation platform OpenFOAM®. Because of its versatility and advanced features such as three-dimensional unstructured grids, dynamic meshes, and high-performance computing, there is a growing

interest in the community to develop mathematical models for solving flow and transport in porous media within OpenFOAM® [53, 54, 55, 38]. We developed a generic interface to combine flow and transport models with existing geochemical packages. We illustrate the versatility of our coupling interface by combining flow models with geochemical models using PHREEQC [56], an open-source and popular geochemistry package that is used in many continuum-scale RTM [57, 58, 59, 60, 61].

In Section 2, we present the mathematical models implemented in *porousMedia4Foam* including a multi-scale and a continuum-scale flow solver, a wide range of porous properties models and the packages used to perform geochemical calculations. In Section 3, we verify the robustness of the coupled hydro-geochemical platform by simulating cases for which reference solutions exist both at the continuum-scale and at the pore-scale. Simulation results are compared with the results obtained with state-of-the-art reactive transport codes. Then in Section 4, we use the simulation framework to illustrate the potential of *porousMedia4Foam* to model hybrid-scale cases.

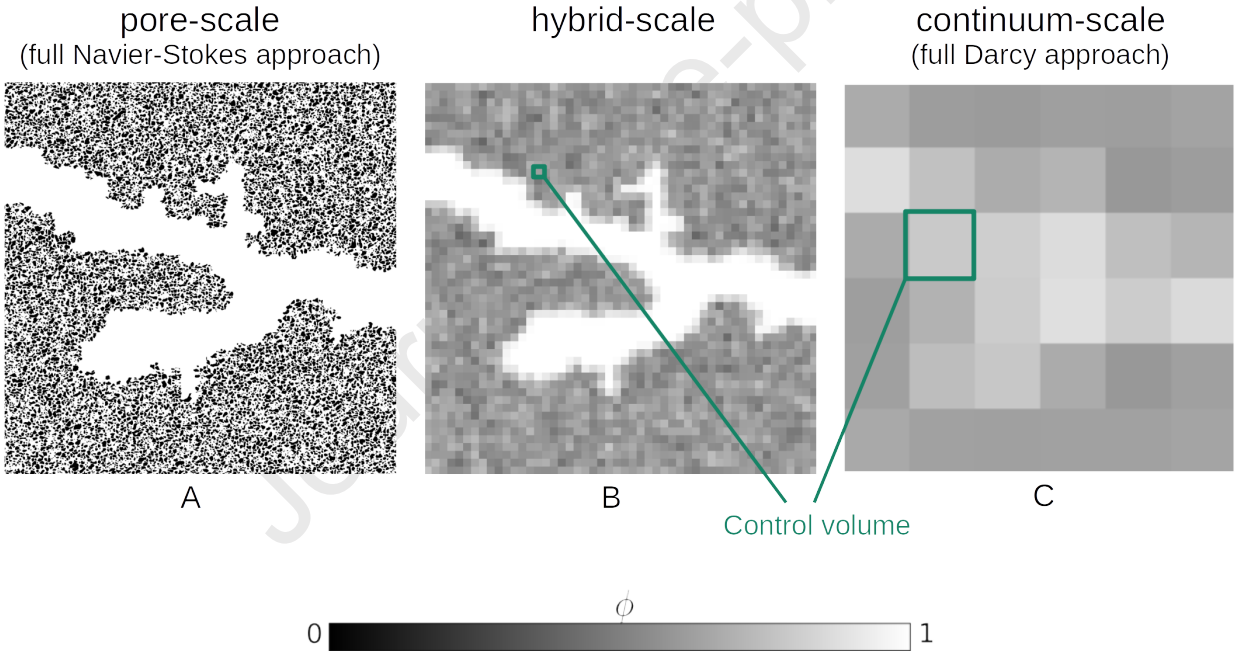

Figure 1: Porosity distribution considered in : *a)* a pure pore-scale approach (Navier-Stokes) for which the porosity is fully resolved, *b)* a micro-continuum approach (DBS) that handles region free of solid and porous region in the same framework, *c)* a pure continuum-scale approach (Darcy) for which all the control volumes contain an aggregate of fluid and solid.

2. The *porousMedia4Foam* package

The multi-scale solver for simulating hydro-geochemical problems is part of *porousMedia4Foam* (https://github.com/csoulain/porousMedia4Foam[1]), a generic platform for solving flow and transport in porous media at various scales of interest. *porousMedia4Foam* is an open-source platform developed by the authors using the C++ library OpenFOAM (http://www.openfoam.org). Hence, the package benefits from all the features of OpenFOAM including the solution of partial differential equations using the finite-volume method on three-dimensional unstructured grids as well as High Performance Computing. Although *porousMedia4Foam* has capabilities for solving two-phase flow (liquid-liquid and liquid-gas) in porous systems, the geochemistry coupling that is introduced in this paper only considers single-phase flow.

The code is organized in three interacting parts: a class that describes porous media properties (Section 2.4), the flow solvers (Section 2.2) and the geochemical packages (Section 2.3). As *porousMedia4Foam* intends to be a versatile platform, it is designed in a such way that other porous media models, other flow solvers or other geochemical packages can be easily implemented using the C++ code architecture. In this section, we introduce the models and their numerical implementation in the code. It is organized as a multiple-entry document in which each model is presented in a self-contained manner so that users can directly refer to the subsection associated with the said model.

2.1. Mineral distribution and porosity

A geological medium is made of an assembly of N_s minerals whose porous properties are defined in Section 2.4. The distribution of each mineral i on the computational grid is determined by the volume fraction,

$$Y_{s,i}\left(x, y, z, t\right) \text{ with } i \in [1, N_s]\,, \tag{1}$$

in each grid block. The N_s solid volume fraction fields are dimensionless. They can be initialized with uniform or distributed values. The evolution of $Y_{s,i}$ due to geochemical reactions is dictated by the geochemical packages that are described in Section 2.3. In some simulations, it is relevant to define an inert mineral $Y_{s,\text{inert}}$ that is not part of the geochemical calculation.

The porosity field is computed by,

$$\phi = 1 - \sum_{i}^{N_s-1} Y_{s,i} - Y_{s,\text{inert}}, \tag{2}$$

and can be updated at any moment following dissolution or precipitation processes. The porosity update at every time-step is optional.

[1]The link is deactivated at the moment. It will be activated as soon as the paper is accepted for publication.

2.2. Flow solvers

porousMedia4Foam for hydro-geochemical simulations includes three flow models: a multi-scale flow solver based on the micro-continuum approach, a continuum-scale Darcy solver and a constant velocity solver (see Table 1).

Table 1: Summary of the flow solvers implemented in *porousMedia4Foam* for simulating hydro-geochemical processes.

Name	Model	Setion	Comments
dbsFoam	Micro-continuum (Darcy-Brinkman-Stokes)	Sec. 2.2.1	pore-scale, hybrid-scale, continuum-scale, Soulaine and Tchelepi [46].
darcyFoam	Darcy's law	Sec. 2.2.1	continuum-scale only.
constantVelocityFoam	constant velocity profile	Sec. 2.2.3	uniform or non-uniform velocity profiles.

2.2.1. *dbsFoam: Multi-scale micro-continuum flow model*

dbsFoam is a multi-scale flow solver based on the micro-continuum modelling approach developed in Soulaine and Tchelepi [46]. Micro-continuum approaches are intermediate between a pure Navier-Stokes description of the transport for which all the porosity is fully resolved (see Fig. 1a), and a pure continuum-scale modelling for which the flow is governed by Darcy's law (see Fig. 1c). This hybrid-scale approach relies on the Darcy-Brinkman-Stokes (DBS) equation [62] that allows for the modelling of flow and transport in regions free of solid and porous regions in a single framework [63, 46]. DBS equation arises from the integration of Navier-Stokes equations over a control volume [64, 65, 66, 67]. The momentum equation reads,

$$\frac{1}{\phi}\left(\frac{\partial \rho_f \boldsymbol{v}_f}{\partial t} + \nabla.\left(\frac{\rho_f}{\phi}\boldsymbol{v}_f\boldsymbol{v}_f\right)\right) = -\nabla p_f + \rho_f \boldsymbol{g} + \nabla.\left(\frac{\mu_f}{\phi}\left(\nabla \boldsymbol{v}_f + {}^t\nabla \boldsymbol{v}_f\right)\right) - \mu_f k^{-1}\boldsymbol{v}_f, \quad (3)$$

where ϕ is the porosity, $\boldsymbol{v}_f$ is the seepage velocity, p_f is the fluid pressure, $\boldsymbol{g}$ is the gravity, ρ_f is the fluid density, μ_f is the fluid viscosity and k is the cell permeability. The porous media properties including porosity and permeability change dynamically with geochemical processes and are updated at every time steps.

Eq. (3) is valid throughout the computational domain regardless the content of a cell. In regions that contain fluid only, $\phi = 1$, and the drag force $\mu_f k^{-1}\boldsymbol{v}_f$ vanishes so that the momentum equation tends to the Navier-Stokes equation. In regions that contain an aggregate of fluid and solid, $0 < \phi < 1$, and the drag force is dominant over the inertial and viscous forces so that Eq. (3) tends asymptotically to Darcy's law.

The momentum equation, Eq. (3), can be used to model pore-scale flows. Indeed, if a solid region is approximated by a low-permeability low-porosity matrix, the velocity in this region goes to near zero which forces a no-slip boundary condition at the fluid/solid interface. This feature of the DBS equation is particularly relevant to solve Navier-Stokes

problems using Cartesian grids only (also called penalized approach) [68, 46] and to move the fluid/solid interface with respect to geochemical processes such as precipitation/dissolution [38, 37] or swelling by using the local porosity field, ϕ, as a phase indicator function [69].

The pressure-velocity coupling is achieved by solving the momentum equation along with the micro-continuum continuity equation for multiple minerals. For an incompressible Newtonian aqueous fluid, the latter reads,

$$\nabla.\boldsymbol{v}_f = \sum_{i=1}^{N_s} \dot{m}_{s,i} \left(\frac{1}{\rho_f} - \frac{1}{\rho_{s,i}} \right), \tag{4}$$

where $\rho_{s,i}$ is the solid density of mineral i and $\dot{m}_{s,i}$ represents the rate of phase change of solid into fluid, or of a fluid into solid. For example, it can represent the rate of solid minerals that is dissolved into aqueous solution. Inversely, it can describe an amount of fluid that is removed of a control volume because it has precipitated. The right-hand side of Eq. (4) is provided by the geochemistry calculation (Section 2.3). Although this term if often neglected in continuum-scale models, it ensures the mass balance at the fluid/solid interface in pore-scale simulations [38], as well as in continuum scale simulations [70].

The flow model formed by Eqs (3)-(4) is discretized using the finite volume method and solved sequentially. The pressure-velocity coupling is handled by a predictor-corrector strategy based on the PIMPLE algorithm implemented in OpenFOAM. It consists in a combination of PISO (Pressure Implicit with Splitting of Operator, Issa [71]) and SIMPLE (Semi-Implicit Method for Pressure Linked Equations, Patankar [72]). PIMPLE algorithm allows both transient and steady-state simulations. Moreover, PIMPLE enables larger time steps than PISO. Further information regarding the numerics is found in Soulaine and Tchelepi [46].

2.2.2. darcyFoam: Darcy's law

darcyFoam is a standard continuum-scale solver that is based on the Darcy's law,

$$\boldsymbol{v}_f = -\frac{k}{\mu_f} \left(\nabla p_f - \rho_f \boldsymbol{g} \right), \tag{5}$$

for describing flow in porous media. Numerically, Eq. (5) is combined along with Eq. (4) to form a Laplace equation solving implicitly for the pressure field, p_f. Then, the velocity field is calculated point-wise using Eq. (5) and p_f. If activatePorosityFeedback is switched on, Darcy's law is recalculated at every time steps to update the velocity and pressure fields according to the new permeability value.

Boundary conditions can be described by imposing fixed pressure or fixed velocity values on the domain edges. However, as darcyFoam solves implicitly for the pressure field, the boundary conditions on the velocity are transformed into pressure gradient conditions using Darcy's law:

$$\boldsymbol{n} \cdot \nabla p_f = -\boldsymbol{n} \cdot \left(\mu_f k^{-1} \boldsymbol{v}_f - \rho_f \boldsymbol{g} \right), \tag{6}$$

where $\boldsymbol{n}$ is the vector normal to the domain boundary. In the code, Eq. (6) is achieved using the boundary condition darcyGradPressure [53].

2.2.3. constantVelocityFoam: Constant flow rate

The flow solver constantVelocityFoam is used to model cases in which the chemical species are transported using a steady-state velocity field, $\boldsymbol{v}_f$ –uniform or non-uniform– provided as an input data that can come from a separate flow simulation. constantVelocityFoam is particularly useful if the feedback between geochemical reactions and the flow is negligible. Indeed, in such a case, the characteristic timescale of flow changes is much longer than the characteristic time of species transport and the calculation of the velocity profile can be decoupled from the species transport.

2.3. Geochemical packages

In *porousMedia4Foam*, complex reaction networks are handled by geochemical packages. The aqueous components are transported using the velocity profile, $\boldsymbol{v}_f$, computed by the flow solver (see section 2.2) and surface reactions rely on the reactive surface area, A_e, calculated with the porous media models (see section 2.4.2). The code architecture of *porousMedia4Foam* is generic so that a wide variety of third-party geochemical packages can be coupled with our platform for solving hydro-geochemical processes at the pore-scale and at the continuum-scale. In this paper, we illustrate the potential of the coupled simulation framework using the popular geochemistry package PHREEQC [73, 56]. Models currently implemented in *porousMedia4Foam* to account for geochemistry are summarized in Table 2.

Table 2: Summary of the geochemical packages implemented in *porousMedia4Foam* for simulating hydro-geochemical processes.

Name	Model	Section	Comments
phreeqcRM	PHREEQC	Sec. 2.3.1	Parkhurst and Wissmeier [56]
simpleFirstOrderKineticMole	first order kinetic, C_i in mol/m^3	Sec. 2.3.2	Molins et al. [37], Soulaine et al. [38]
transportOnly	no geochemistry	Sec. 2.3.3	–
flowOnly	no transport, no geochemistry	Sec. 2.3.4	–

The geochemical packages update the water composition, C_j and the distribution of the solid minerals $Y_{s,i}$, and return the rate of solid changes,

$$\dot{m}_{s,i} = -\frac{\partial \rho_{s,i} Y_{s,i}}{\partial t}, \tag{7}$$

where $\rho_{s,i}$ is the density of solid mineral i.

2.3.1. phreeqcRM

The phreeqcRM class calls the general-purpose geochemical reaction model PHREEQC through the PhreeqcRM module. It carries out the transport of the aqueous solution composition, C_j (in mol/kg$_{\text{water}}$), along with equilibrium and kinetic reactions with the solid minerals described by $Y_{s,i}$. phreeqcRM is set with components, i.e. SOLUTION_MASTER_SPECIES total concentration.

The geochemistry setup is carried out using an input file that follows PHREEQC format. Hence, the aqueous composition is defined in the block SOLUTION (0 for the composition of the injected fluid at the inlet boundary, 1 for the initial aqueous composition in the bulk). The EQUILIBRIUM_PHASES and KINETICS blocks are generated automatically within the code and the user only has to assign before the calculation which mode of reactions is used for each mineral. Moreover, *porousMedia4Foam* can load any customized database using PHREEQC format.

The coupling between transport and reactions relies on an operator-splitting approach based on the Strang's algorithm [74]. First, all species concentration fields, C_j, are transported sequentially using the advection-dispersion equations,

$$\frac{\partial \phi C_j}{\partial t} + \nabla \cdot (\boldsymbol{v}_f C_j) - \nabla \cdot \left(\phi \mathsf{D}_j^* . \nabla C_j\right) = 0, \tag{8}$$

where $\boldsymbol{v}_f$ is the fluid velocity computed with the flow solver (see Section 2.2) and D_j^* is an effective diffusion tensor that accounts for tortuosity and hydrodynamic dispersion effects (see Section 2.4.3). The transport equation is discretized on the computational domain using the finite-volume method and solved implicitly using OpenFOAM's engines.

Then, the volume fractions of solid minerals, $Y_{s,i}$, are updated according to phase equilibrium and/or kinetic reaction calculations provided by PHREEQC. Reaction kinetics use the surface area computed at every time steps using the surface area models in section 2.4.2. It corresponds to the surface area per volume and its units are $\mathrm{m}^2/\mathrm{m}^3$ (or m^{-1}). Hence, the RATE block provided in PHREEQC database to describe reaction rates has to be defined accordingly.

2.3.2. simpleFirstOrderKineticMole

simpleFirstOrderKineticMole is a simple geochemical engine for solving the transport of a single species labelled A that reacts with solid minerals using first order kinetic reactions. It is an extension to multiple minerals of the model used in the benchmark presented in [37] in which pore-scale simulators were used to model the dissolution of a calcite crystal by hydrochloric acid.

The chemical reaction reads,

$$\mathrm{Mineral}_{i(s)} + \mathrm{A} = \mathrm{B}_i. \tag{9}$$

The mass balance equation for species A reads,

$$\frac{\partial \phi C_A}{\partial t} + \nabla \cdot (\boldsymbol{v}_f C_A) - \nabla \cdot \left(\phi \mathsf{D}_j^* . \nabla C_A\right) = -\left(\sum_{j=1}^{N_s} A_{s,j} \left(k_{j,A}\gamma_A\right)\right) C_A, \tag{10}$$

where $\boldsymbol{v}_f$ is the fluid velocity, D_j^* is an effective diffusion tensor, $A_{s,j}$ is the reactive surface area of mineral j (in m^{-1}), and $(k_{j,A}\gamma_A)$ is the constant of reaction of the species A with the mineral j (in m/s) following the notations adopted in [37]. In simpleFirstOrderKineticMole, the concentration field, C_j, is defined in $\mathrm{mol}/\mathrm{m}^3$. The equation is discretized on the computational grid using the finite-volume method and solved implicitly.

The distribution of solid minerals evolves according to,

$$\frac{\partial Y_{s,i}}{\partial t} = -A_{s,A}\left(k_{i,A}\gamma_A\right) V_{m_{s,i}} C_A, \tag{11}$$

where $V_{m_{s,i}}$ (in m^3/mol) is the molar volume of the reacting mineral.

2.3.3. *transportOnly*

transportOnly solves the advection-dispersion equation,

$$\frac{\partial \phi C_j}{\partial t} + \nabla \cdot (\boldsymbol{v}_f C_j) - \nabla \cdot \left(\phi \mathsf{D}_j^* . \nabla C_j\right) = 0, \tag{12}$$

without considering geochemistry. It allows the transport of species using the dispersion models implemented in *porousMedia4Foam* (see Table 5).

2.3.4. *flowOnly*

flowOnly is an empty class for computing velocity profiles without species transport nor geochemistry. For example, Poonoosamy et al. [11] used the multi-scale flow solver of *porousMedia4Foam* to compute the steady-state velocity profile in absence of geochemical reactions within a two-scale domain, i.e. a domain that contains both solid-free regions and porous regions (see Fig. 1b). This option is particularly interesting in cases for which geochemistry and flow can be treated independently from each other.

2.4. Porous media models

The flow solvers and geochemistry modules rely on porous media properties including absolute permeability, specific surface area and dispersion tensor. These properties describe pore-scale effects related to the micro-structure geometry of the porous medium. Hence, they may change if the micro-structure evolves with geochemical reactions.

2.4.1. Absolute permeability models

The absolute permeability describes the ability of a porous medium to conduct the flow. This property is intrinsic to the medium micro-structure and therefore evolves with geochemical processes including precipitation and dissolution. *porousMedia4Foam* includes several porosity-permeability relationships summarized in Table 3.

2.4.2. Surface area models

The estimation of the reactive surface area is crucial to model geochemical processes described by kinetic reactions. Actually, reactive surface area is a difficult quantity to assess as only a portion of the geometric surface area is accessible to the reactants. For example, in an advection-dominated transport, only the surfaces at the vicinity of the faster flowlines react [38] leading to a reactive surface area smaller than the geometric surface area. Moreover, the evolution of the specific surface area as the mineral volume fractions change due to dissolution or precipitation is not necessarily monotonic [79]. Table 4 summarizes the models

Name	Expression	Comments
none	$k = 0$	–
constant	$k = k_0$	k_0 is uniform or non-uniform.
Power-law	$k = k_0 \left(\frac{\phi}{\phi_0}\right)^n$	n is a user defined variable.
Kozeny-Carman	$k = k_0 \left(\frac{\phi}{\phi_0}\right)^n \left(\frac{1-\phi_0}{1-\phi}\right)^m$	by default, $n = 2$ and $m = 3$ [75, 76].
Verma-Pruess	$k = k_0 \left(\frac{\phi-\phi_c}{\phi_0-\phi_c}\right)^n$	n is a model parameter. ϕ_c refers to the critical porosity where permeability reduces to 0 [77].
Hele-Shaw	$k = \frac{h^2}{12}$	for simulating 2D depth-averaged flow in micromodels (e.g. Poonoosamy et al. [11], Roman et al. [78]).

Table 3: Summary of the permeability-porosity models implemented in *porousMedia4Foam*. In the table, subscripts 0 refers to variable data at initial time. Optionally, ϕ_0 and k_0 are updated at every time-steps.

implemented in *porousMedia4Foam* to describe the surface area as a function of the mineral volume fraction.

Unlike continuum-scale simulations, the surface area in pore-scale modelling is not an input parameter but is a direct output of the simulation. Indeed at the pore-scale, the micro-structure of the porous medium is fully resolved in the computational grid and there is a sharp interface between the fluid and the solid mineral. The Volume-of-Solid model computes the surface area of an explicit fluid/solid interface using the gradient of the volume fraction of mineral (see Soulaine et al. [38] for additional details on the technique).

2.4.3. Dispersion models

In porous media, the spreading of a solute is not governed only by molecular diffusion (D_i) but also by the micro-structure and the local velocity field. On the one hand, the tortuosity of the porous structure tends to slow down the spreading. On the other hand, hydrodynamic dispersion stretches a solute band in the flow direction during its transport. In *porousMedia4Foam*, a single effective diffusion tensor, D_i^*, is used to represent both mechanisms. The models implemented in the code are summarized in Table 5.

3. Verification of the hydro-geochemical simulation platform

In this section, the multi-scale hydro-geochemical simulation package *porousMedia4Foam* introduced in Section 2 is used along with PHREEQC to investigate several scenarios for which reference solutions exist. The verification of the results is achieved by comparison against benchmarks published in literature both at the continuum-scale and at the pore-scale. Essential files required to run all the test cases presented in this section are available as examples within the package. All simulations were run on Intel Xeon with 2.60 GHz.

Table 4: Summary of the specific surface area models implemented in *porousMedia4Foam*. Units of specific surface area are m^{-1}.

Name	**Expression**	**Comments**
None	$A_s = 0$	If specific surface area is not necessary, e.g. for phase equilibrium calculation.
Constant	$A_s = A_0$	–
Volume of solid	$A_s = \lvert\nabla Y_s\rvert\,\psi$	for pore-scale simulations only. Compute the local surface area based on the mineral mapping. ψ is a diffuse interface function [38].
Power-law	$A_s = A_0\,(Y_s)^n$	n is a user defined variable
Sugar-lump	$A_s = \left(A_0 + A_m\left(1-\left(\frac{Y_s}{Y_0}\right)^{n_1}\right)^{n_2}\right)\left(\frac{Y_s}{Y_0}\right)^{n_3}$	Evolution of the surface area of an aggregate during dissolution [79]. A_m is the maximum surface area given by the sum of the surface areas of all individual particles, n_1, n_2 and n_3 are user-defined parameters.
Hydro-geochemical coupling	$A_s = A_0\left(\frac{Y_s}{Y_0}\right)^n\left(1-\exp\left(Pe^{-p}Da^{-q}\right)\right)$	including surface reduction due to hydro-geochemical coupling [38]. n, p, q are user defined parameters.

Table 5: Summary of the dispersion models implemented in *porousMedia4Foam*. I is the unit tensor.

Name	**Expression**	**Comments**
none	$\mathsf{D}_i^* = \mathsf{0}$	for modelling transport by advection only
diffusionOnly	$\mathsf{D}_i^* = D_i\mathsf{I}$	no tortuosity effects, no hydrodynamic dispersion.
archiesLaw	$\mathsf{D}_i^* = \phi^n D_i\mathsf{I}$	tortuosity is represented by ϕ^n. By default, $n = 0$
linearDispersion	$\mathsf{D}_i^* = \phi^n\left(\left(D_i + \alpha_T\lvert\boldsymbol{v}\rvert\right)\mathsf{I} + \frac{(\alpha_L-\alpha_T)}{\lvert\boldsymbol{v}\rvert}\boldsymbol{vv}\right)$	tortuosity is represented by ϕ^n. α_L and α_L are model parameters describing lateral and longitudinal dispersion respectively.

3.1. *Verification at the continuum-scale*

We verify the ability of *porousMedia4Foam* to simulate coupled hydro-geochemical processes that include porosity feedback on the transport properties at the continuum-scale. We also verify that the multi-scale solver dbsFoam tends asymptotically towards Darcy's law in porous domains. The case is based on the Benchmark 1 described in Xie et al. [13]. It consists of a 2 meters long 1D column initially filled with 35 % of inert mineral and 30 % of calcite. An acid (pH = 3) is continuously injected at the inlet to initiate the dissolution of calcite according to,

$$\begin{aligned} \mathrm{CaCO_3} + \mathrm{H^+} &\leftrightarrow \mathrm{Ca^{2+}} + \mathrm{HCO_3^-}, \\ \mathrm{HCO_3^-} &\leftrightarrow \mathrm{H^+} + \mathrm{CO_3^{2-}}. \end{aligned} \tag{13}$$

Table 6 provides the initial and boundary conditions data specific to the primary components. A difference of 0.007 m in hydraulic head is applied between the inlet and outlet [13] by fixing the pressure at 70 Pa and 0 Pa respectively at the inlet and outlet boundaries throughout the simulation.

Primary components	Units	Initial conditions	Boundary condition
pH	-	9.38	3
-	-	9.38	3
Ca	$\mathrm{mol/kg_{water}}$	1.56×10^{-4}	9.97×10^{-5}
C(4)	$\mathrm{mol/kg_{water}}$	2.56×10^{-4}	9.97×10^{-3}
S(6)	$\mathrm{mol/kg_{water}}$	9.97×10^{-11}	6.44×10^{-4}

Table 6: Initial and boundary conditions of the primary components for calcite dissolution under kinetic conditions considering porosity feedback.

The calcite dissolution with porosity feedback is simulated using both the multi-scale solver dbsFoam and the continuum-scale solver darcyFoam. The aqueous species are transported by advection only. The calcite dissolution is modelled using a kinetic rate of reaction with $k_{\mathrm{calcite}} = 5 \times 10^{-5}\,\mathrm{mol/m^2/s}$ and the initial specific area $A_0 = 1\,\mathrm{m^2/m^3}$. As the calcite dissolves, the surface area decreases according to a power-law function with $n = 2/3$ (see Table 4). The porosity-permeability relationship is described by the Kozeny-Carman equation (Table 3). The initial permeability of the column is set to $k_0 = 1.186 \times 10^{-11}\,\mathrm{m^2}$. The column is spatially discretized with $\Delta x = 25\,\mathrm{mm}$ (80 cells). 150 years are simulated with $\Delta t = 21600\,\mathrm{s}$.

There is a perfect match between dbsFoam and darcyFoam confirming that the multi-scale solver converges well to the continuum-scale solution predicted by Darcy's law (Figure 2). The analysis of results includes the evolution of porosity (Fig. 2a), calcite volume fraction (Fig. 2b), hydraulic head (Fig. 2c) along the column length and the outflux over time (Fig. 2d). To be consistent with the benchmark of [13], we consider the cross-sectional area of the column to be $1\,\mathrm{m^2}$. As the dissolution of calcite occurs, the calcite volume fraction decreases and the porosity increases over time. In Fig. 2c, we notice different slopes of hydraulic head at different times. The slope is minimal where porosity is large and vice-versa.

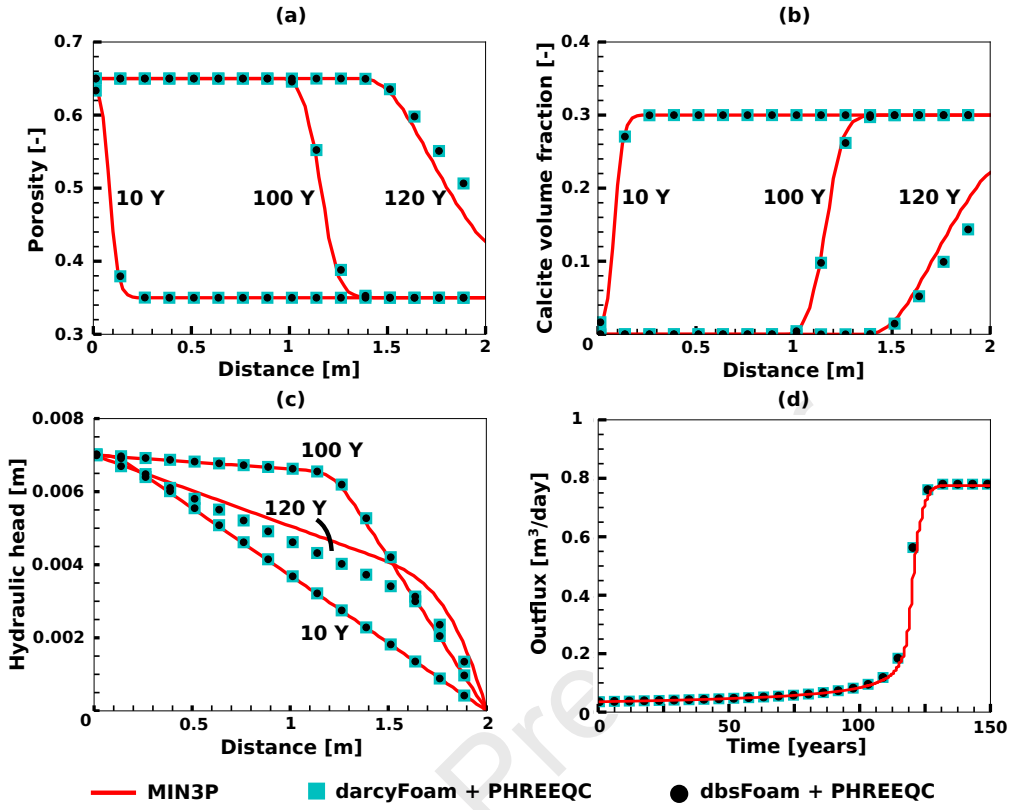

Figure 2: Calcite dissolution under kinetic conditions considering feedback of porous media properties. Evolution of (a) porosity, (b) calcite volume fraction, (c) hydraulic head along the channel and (d) evolution of outflux. MIN3P data is from [13] for comparison.

The velocity – and therefore the outflux – increases over time as the permeability (and porosity) of the system increases. The evolution of porosity, calcite volume fraction, hydraulic head and outflux predicted by *porousMedia4Foam* solvers are in close agreement with those of MIN3P which demonstrates the ability of our platform to simulate hydro-geochemical processes with porosity feedback.

3.2. Verification at the pore-scale

In this section, we highlight the capabilities of our OpenFOAM package to model hydro-geochemical interactions occurring at the pore-scale using PHREEQC.

In *porousMedia4Foam*, pore-scale simulations are run using the micro-continuum approach through the flow solver dbsFoam. At the pore-scale, the reaction rates are directly applied at the fluid-mineral interface that is described explicitly in the computational grid using the mineral volume fraction. The micro-continuum approach has been used to simulate the dissolution of a calcite crystal at the pore-scale and compared successfully with microfluidic experiments [38]. In Molins et al. [37], the approach is compared with state-of-the-art RTM at the pore-scale using various numerical techniques including Chombo-Cruch with Level-Set [20], Lattice Boltzmann Method [80], dissolFoam moving grids with confor-

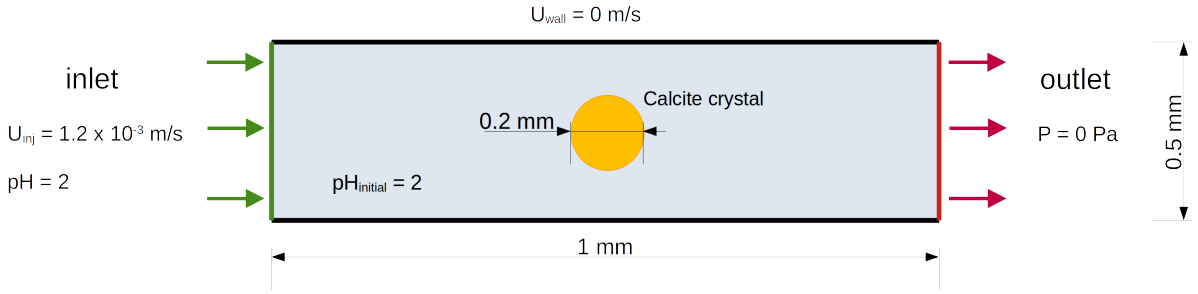

Figure 3: The considered model set-up along with initial and boundary conditions to investigate calcite grain dissolution in a microchannel.

mal mapping [81], and Vortex methods [82]. The benchmark consists of a 0.2 mm diameter calcite crystal posted in a 1 mm long 0.5 width channel (see Fig. 3). An acidic solution of pH=2 is continuously injected from the inlet at a rate of $U_{\text{inj}} = 1.2 \times 10^{-3}\,\text{m/s}$. The calcite crystal dissolution is described considering a kinetic rate,

$$r = A_{\text{calcite}}\,(k_{\text{calcite}}\gamma)\,c_{H^+}, \tag{14}$$

where r is the reaction rate in $\text{mol/m}^3\text{/s}$, A_{calcite} is the reactive surface area in m^2/m^3 computed using the volume-of-solid approach (see Table 4), $(k_{\text{calcite}}\gamma) = 0.89 \times 10^{-3}\,\text{m/s}$ is the reaction rate constant of calcite and, c_{H^+} is the concentration of H^+ in mol/m^3. This reaction rate may not be fully representative of the underlying geochemical processes. It has been chosen in Molins et al. [37] to demonstraste the ability of various approaches to move the fluid-mineral interface according to geochemical processes. All the numerical methods were able to capture accurately the shape evolution of the calcite crystal, giving confidence in pore-scale simulators for moving fluid-mineral interfaces along with geochemical processes.

Actually, in Soulaine et al. [38] and Molins et al. [37], the micro-continuum approach, dbsFoam, was combined with the geochemical package simpleFirstOrderKineticsMole (see Table 2) that solves Eq. (14) using OpenFOAM's internal engines. This limits drastically the applicability of the approach to comprehensive reaction networks. In this section, we reproduce the two-dimensional case presented in Molins et al. [37] using dbsFoam and phreeqcRM to demonstrate the robustness of our coupling between OpenFOAM and PHREEQC at the pore-scale. The kinetic rate in PHREEQC input file has been modified to match Eq. (14). The system is spatially discretized using a Cartesian mesh of 128×64 cells. The simulation is run for 45 minutes using a time step size $\Delta t = 5\,\text{ms}$.

The shape evolution of the calcite grain determined by the two approaches matches perfectly (Fig. 4) which verifies, therefore, that in our modelling plateform, PHREEQC can be used to model hydro-geochemical interactions occurring at the pore-scale. This gives us confidence for further investigations that rely on more complex reactive transport phenomena occurring at the pore-scale.

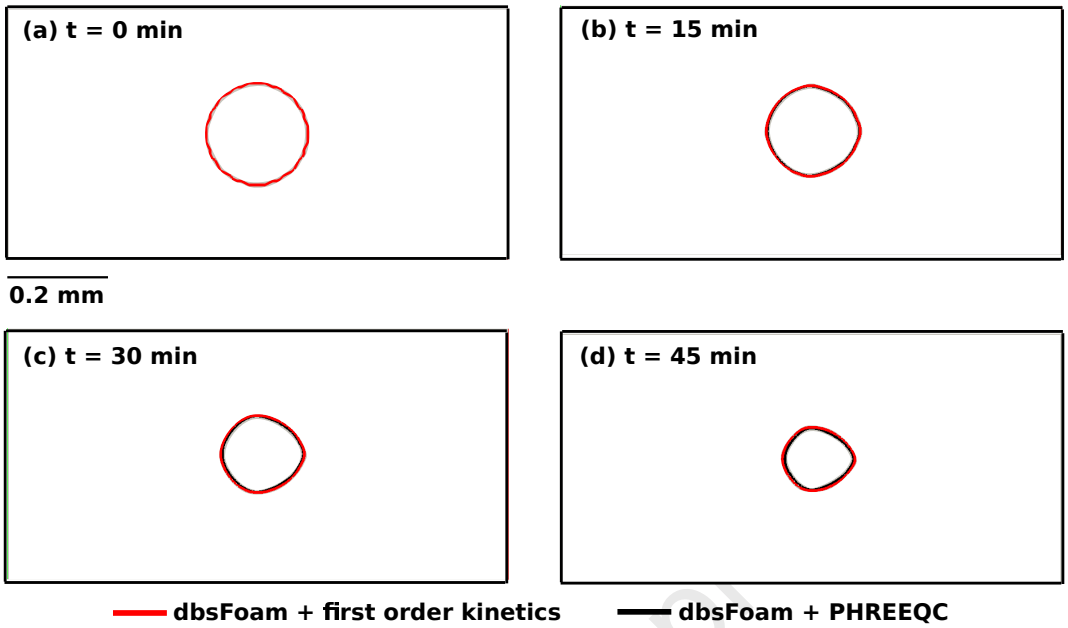

Figure 4: Evolution of the shape of the calcite grain as a function of time ((a) t = 0 min, (b) t = 15 min, (c) t = 30 min and (d) t= 45 min) predicted by dbsFoam + first order kinetics geochemical module (simpleFirstOrderKineticsMole, red line) and dbsFoam + PHREEQC (phreeqcRM geochemical module of *porousMedia4Foam*, black line). The red and black lines represent cells having calcite volume fraction of 0.5.

4. Hybrid-scale simulation in fractured porous media

In most subsurface environments, fractures intercept porous media domains. These fractures act as free-flow zones transporting substantial quantities of fluids alongside chemical species compared to the flow and transport that occur within the porous medium [83, 84]. The complex interplay between advection, diffusion, and reaction can lead to very different dissolution and precipitation patterns. For example, Poonoosamy et al. [11] uses micro-Raman spectroscopy to visualise the replacement of celestite with barite in a fractured porous media flooded with a solution that contains barium ions. They observe that the mineral replacement occurs either uniformly or at the vicinity of the fracture-matrix interface. This difference in the mineral distribution was attributed to the injection flow rates leading to advection or diffusion-dominated transport.

We investigate such a multiscale system, where a fracture is sandwiched in between a reactive porous matrix made of 50% celestite ($SrSO_4$) having specific reactive surface area of $A_0 = 20000\,\mathrm{m}^2/\mathrm{m}^3$ as shown in Fig. 5. The fracture has a length of $\ell = 0.03\,\mathrm{m}$ and height $h = 0.002\,\mathrm{m}$. Transport phenomena in the fracture is fully resolved, i.e. the flow is governed by Navier-Stokes equations whereas the flow in the matrix is described by Darcy's law. This hybrid-scale case is modelled using the dbsFoam solver. The initial porosity and permeability of the porous medium are $\phi_0 = 0.5$ and $k_0 = 10^{-12}\,\mathrm{m}^2$, respectively. A solution containing $300\,\mathrm{mol}/\mathrm{m}^3$ of barium (Ba^{2+}) is continuously injected through the inlet at a constant velocity U_{inj} for 200 hours. The dispersivity of species within the porous matrix are

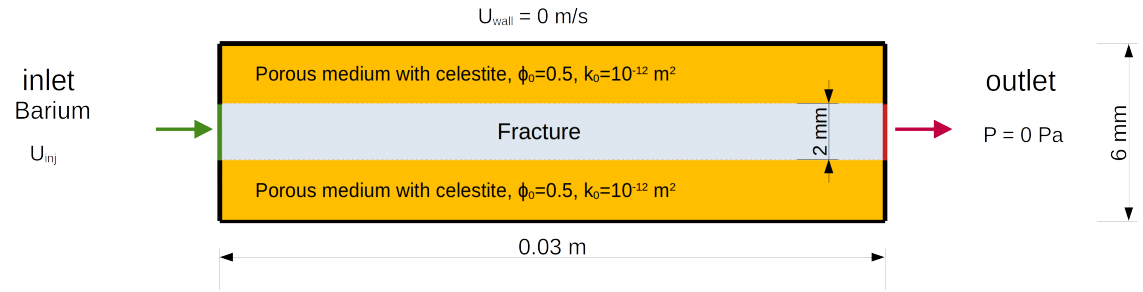

Figure 5: Numerical set-up for the hybrid-scale case study. A fracture is sandwiched in between two layers of reactive porous medium. The reactive porous medium comprises of celestite. Barium is injected at the inlet. We investigate this scenario considering two different injection velocities, $U_{\text{inj}} = 10^{-2}\,\text{m/s}$ and $U_{\text{inj}} = 10^{-6}\,\text{m/s}$.

taken into account considering linear dispersion law (Table 5) with molecular diffusion set to $D_j = 10^{-9}\,\text{m}^2/\text{s}$, hydrodynamic dispersion coefficient set to $\alpha_L = 10^{-5}\,\text{m}$ and tortuosity exponent set to $n = 2$. Once the barium ions reach the porous matrix, celestite dissociates into strontium (Sr^{2+}) and sulphate (SO_4^{2-}) ions. The barium ions react with sulphate ions resulting in the precipitation of barite ($BaSO_4$) according to the following reaction [85],

$$Ba^{2+} + SrSO_4 \rightarrow BaSO_4 + Sr^{2+}. \tag{15}$$

Celestite dissolution is taken into account considering kinetics with $k_{\text{celestite}} = 10^{-5.66}\,\text{mol/m}^2/\text{s}$ whereas, barite precipitation is accounted considering phase equilibrium. Celestite reactive surface area evolves linearly with its volume fraction. The matrix permeability is updated according to Kozeny-Carman.

We investigate the ongoing hydrogeochemistry within this system considering two different injection velocities, $U_{\text{inj}} = 10^{-2}\,\text{m/s}$ and $U_{\text{inj}} = 10^{-6}\,\text{m/s}$. The Pclet number, $Pe = U_{\text{inj}}\ell/D_j$ (where the reference length-scale is the fracture aperture), characterizes the importance of advection with respect to diffusion within the fracture. The highest velocity corresponds to advection-dominated transport ($Pe \approx 10^4$) while the lowest corresponds to diffusion-dominated regime ($Pe \approx 1$). For both cases, the second Damkhler number that determines the timescale of reaction with respect to the timescale of species diffusion at the mineral surface is $\text{Da}_{II} = k_{\text{celestite}}\ell/(c_{Ba^{2+}} D_j) \approx 3.6 \times 10^{-4}$ (where the reference length-scale is the inverse of the specific surface area, $\ell = A_0^{-1}$, according to Soulaine et al. [38]).

We notice differences in the pattern of celestite dissolution and barite precipitation whether the transport in the fracture is dominated by advection or by diffusion in agreement with Poonoosamy et al. [11] observations (Fig. 6). For advection dominated regime ($Pe > 1$), there are two characteristic timescales for the solute transport: first, the barium ions flow through the fracture by advection, then they diffuse laterally into the matrix. Because of the timescale contrast between the two processes, the concentration profile of barium ions is uniform along the porous matrix which leads to a uniform pattern of celestite dissolution and barite precipitation as seen in Figs. 6 and 7. For diffusion-dominated regimes ($Pe \leq 1$), the characteristic transport timescales both in the fracture and in the matrix are of the same order of magnitude. Therefore, the front of barium ions in the matrix follows the

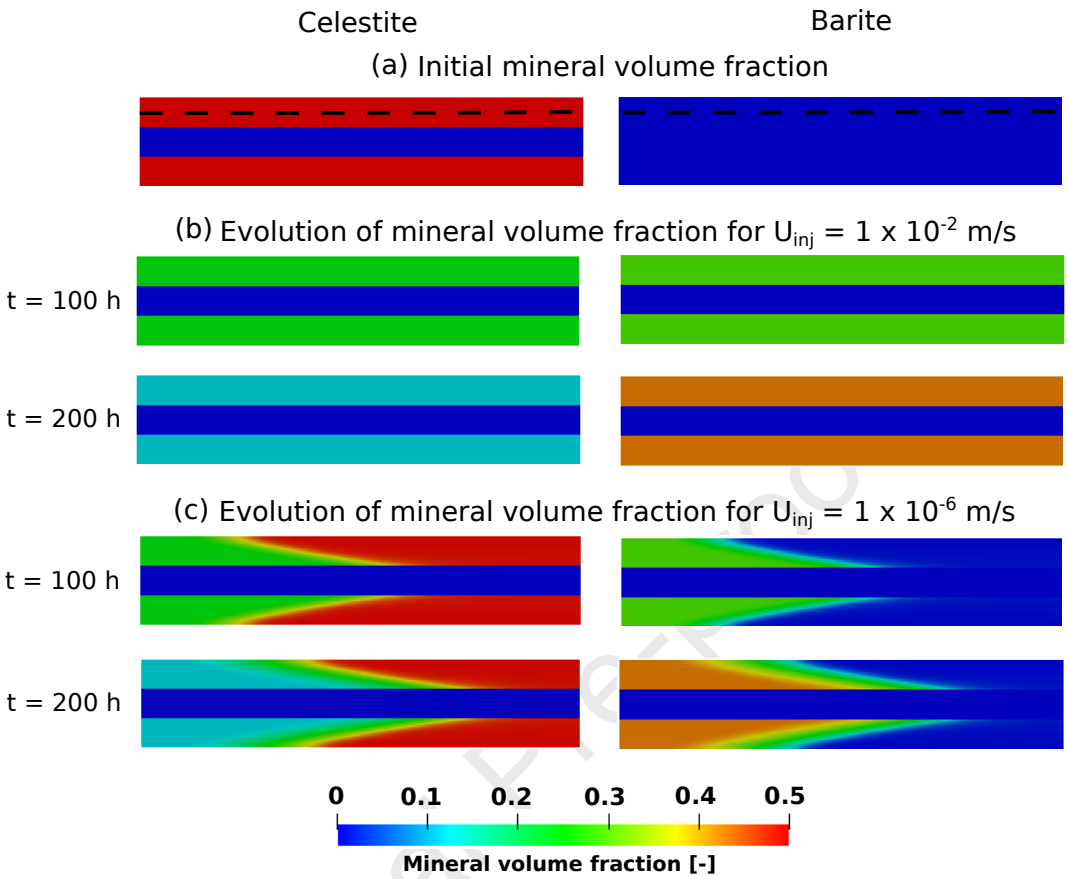

Figure 6: Evolution of mineral volume fractions - celestite on the left and barite on the right - at different injection velocities. (a) Initial (t = 0 s) mineral volume fractions. (b) Mineral volume fractions at 100 h and 200 h for $U_{\text{inj}} = 1 \times 10^{-2}$ m/s, and (c) mineral volume fractions at 100 h and 200 h for $U_{\text{inj}} = 1 \times 10^{-6}$ m/s.

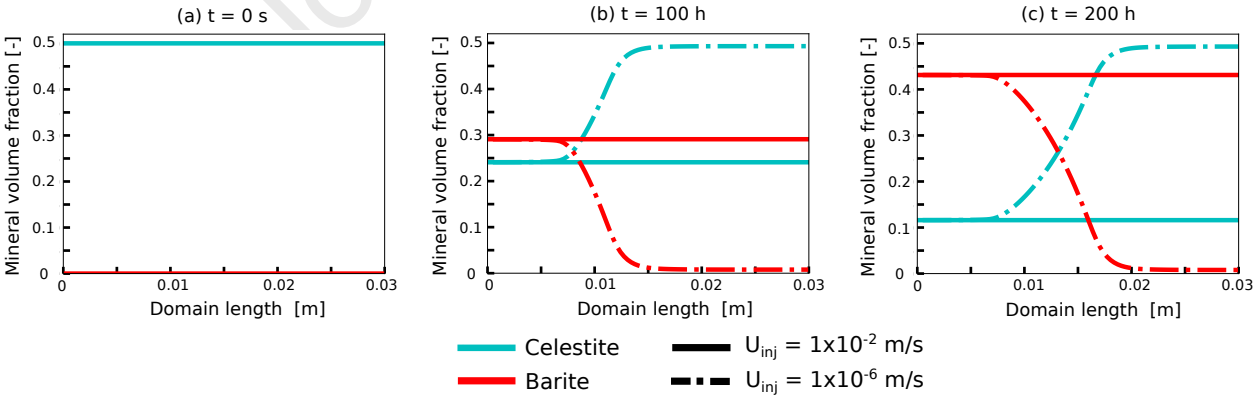

Figure 7: Plots comparing the mineral volume fractions of celestite and barite at three different time intervals (a) t = 0 s, (b) t = 100 h and (c) t = 200 h for different injection velocities. The mineral volume fraction data is collected along the length of the domain at a distance of 0.001 m from the top wall boundary as highlighted by dashed black line in Fig. 6 (see initial mineral volume fraction).

diffusive front within the fracture. Subsequently, we observe mineral dissolution (celestite) and precipitation (barite) fronts within the porous matrix (Figs. 6 and 7).

This illustration emphasizes the capabilities of *porousMedia4Foam* to model dual-porosity systems in reactive environments using hybrid-scale approach. Our platform is therefore a powerful tool to complement and augment reactive transport experiments including high-resolution imaging of the evolution the fracture aperture including the effect of the weathered zone [83, 79, 84, 86] and two-scale reactive microfluidic experiments [11, 87, 88].

In a logic of cascade of scales nested within each other, fractured porous media can be modelled by: *i)* pore-scale approaches, *ii)* discrete fracture networks, *iii)* dual porosity models. The hybrid-scale approach that we propose in this paper is intermediate between a full pore-scale description in which the fracture and the pores in the matrix are fully resolved and a discrete fracture network in which the matrix is modelled as a porous medium and the fractures as discrete elements that exchange matter with the matrix. The hybrid-scale approach is therefore crucial to characterize and improve the effective parameters (e.g. transfer functions between the porous matrix and the fracture) used in discrete fracture networks and larger-scale models.

5. Conclusion

We developed an integrated open-source simulator to model hydro-geochemical processes at various scales of interest including pore-scale and reservoir-scale. The simulation platform is part of *porousMedia4Foam*, a package that solves flow and transport in porous media using the open-source library OpenFOAM. The modelling framework handles complex reactions network as a function of flow conditions, water composition and minerals distribution within the rock including the complex porosity feedback between flow and chemistry. Moreover, *porousMedia4Foam* benefits from all features of OpenFOAM libraries. Hence, the code is fully parallel and handles structured as well as unstructured grids in one, two and three dimensions. The interface between the flow simulator and the geochemistry is generic and can be used to couple a large variety of geochemical packages. In this paper, we illustrated the hydro-geochemical capabilities of the coupled solver using PHREEQC.

Unlike other reactive transport simulators, *porousMedia4Foam* is multi-scale, i.e. a unique flow solver describes transport processes both at the continuum-scale and the pore-scale. Importantly, the two scales can be solved simultaneously in geological formations that feature large contrast of permeability and porosity. For example, in fractured rocks, *porousMedia4Foam* solves Stokes flow in the fracture network and Darcy's law in the porous matrix. This multi-scale model is achieved using the micro-continuum approach, hybrid-scale approach based on the Darcy-Brinkman-Stokes equation. Indeed, this approach is intermediate between a pure Navier-Stokes description of the transport for which all the porosity is fully resolved and pure continuum-scale modeling based on Darcys law. Besides this hybrid-scale approach, *porousMedia4Foam* also includes a standard Darcy solver for continuum-scale simulations. Therefore, the same simulator can be used to simulate flow, transport, and geochemical reactions in an reservoir and in 3D micro-tomography images.

The coupled hydro-geochemical simulator was verified by running cases for which reference solutions exist. These solutions are well-established and used in the reactive transport community to benchmark state-of-the-art codes available both at the continuum-scale [13] and at the pore-scale [37]. Finally, we demonstrated the ability of our advanced modelling framework to simulate dissolution and precipitation processes in fractured porous media at the pore-scale using the hybrid-scale approach. Here, the reactive medium consisted of celestite grains that reacted with a barium chloride solution injected into the system, leading to the dissolution of celestite and the growth of barite. We observed differences in mineral precipitation - dissolution patterns by varying the injection rates.

Because *porousMedia4Foam* has already capabilities for modelling two-phase flow in porous media both at the pore- and Darcy's scales using two-phase micro-continuum technique [52, 89, 90], true multiscale and multiphase RTM is envisioned to be implemented in *porousMedia4Foam* framework.

Software and Data Availability

porousMedia4Foam, the software introduced in this paper is built using open-source libraries including OpenFOAM and PHREEQC. The source code and the cases presented in the paper are available on GitHub (`https://github.com/csoulain/porousMedia4Foam`[2]).

Contributions of the authors

CS is the *porousMedia4Foam* architect. CS and SP implemented new models in *porousMedia4Foam* and corrected bugs. SP and CT designed and setup the benchmark problems. SP run the simulations. CS, SP, CT and FC discussed, interpreted the results and wrote the paper. CS, CT and FC applied for funding.

Acknowledgments

The research leading to these results has received funding from the French Agency for Research (Agence Nationale de la Recherche, ANR) through the labex Voltaire ANR-10-LABX-100-01, the grant CATCH ANR-18-CE05-0035, and through the FraMatI project under contract ANR-19-CE05-0002. It has also received financial support from the CNRS through the MITI interdisciplinary programs. This project has received funding from the European Unions Horizon 2020 research and innovation programme under grant agreements No 847593 (WP DONUT) and No 850626 (REFLECT Project). SP postdoctoral fellowship was funded by BRGM through the PORE-REACTIF project from the Alliance Nationale de Coordination de la Recherche pour lEnergie (ANCRE). The authors benefitted from the use of the cluster at the Centre de Calcul Scientifique en rgion Centre-Val de Loire.

[2]The link is deactivated at the moment. It will be activated as soon as the paper is accepted for publication.

[1] C. Steefel, C. Appelo, B. Arora, D. Jacques, T. Kalbacher, O. Kolditz, V. Lagneau, P. Lichtner, K. U. Mayer, J. Meeussen, et al., Reactive transport codes for subsurface environmental simulation, Computational Geosciences 19 (3) (2015) 445–478.

[2] L. Li, K. Maher, A. Navarre-Sitchler, J. Druhan, C. Meile, C. Lawrence, J. Moore, J. Perdrial, P. Sullivan, A. Thompson, et al., Expanding the role of reactive transport models in critical zone processes, Earth-science reviews 165 (2017) 280–301.

[3] D. J. DePaolo, D. R. Cole, Geochemistry of geologic carbon sequestration: an overview, Reviews in Mineralogy and Geochemistry 77 (1) (2013) 1–14, doi:10.2138/rmg.2013.77.1.

[4] F. Claret, N. Marty, C. Tournassat, Modeling the Long-term Stability of Multi-barrier Systems for Nuclear Waste Disposal in Geological Clay Formations, chap. 8, John Wiley & Sons, Ltd, ISBN 9781119060031, 395–451, doi:https://doi.org/10.1002/9781119060031.ch8, URL https://onlinelibrary.wiley.com/doi/abs/10.1002/9781119060031.ch8, 2018.

[5] P. C. Lichtner, Continuum model for simultaneous chemical reactions and mass transport in hydrothermal systems, Geochimica et Cosmochimica Acta 49 (3) (1985) 779–800.

[6] K. U. Mayer, E. O. Frind, D. W. Blowes, Multicomponent reactive transport modeling in variably saturated porous media using a generalized formulation for kinetically controlled reactions, Water Resources Research 38 (9) (2002) 13–1.

[7] T. Xu, E. Sonnenthal, N. Spycher, K. Pruess, TOUGHREACTA simulation program for non-isothermal multiphase reactive geochemical transport in variably saturated geologic media: Applications to geothermal injectivity and CO2 geological sequestration, Computers & Geosciences 32 (2) (2006) 145 – 165, ISSN 0098-3004, doi:https://doi.org/10.1016/j.cageo.2005.06.014, URL http://www.sciencedirect.com/science/article/pii/S0098300405001500.

[8] P. C. Lichtner, G. E. Hammond, C. Lu, S. Karra, G. Bisht, B. Andre, R. Mills, J. Kumar, PFLOTRAN User Manual: A Massively Parallel Reactive Flow and Transport Model for Describing Surface and Subsurface Processes, Tech. Rep., United States, URL https://www.osti.gov/servlets/purl/1168703, 2015.

[9] D. Jacques, J. Simunek, D. Mallants, M. T. Van Genuchten, Modeling coupled hydrologic and chemical processes: Long-term uranium transport following phosphorus fertilization, Vadose Zone Journal 7 (2) (2008) 698–711.

[10] J. Bear, Dynamics of fluids in porous media, Elsevier, New York, URL Dynamicsoffluidsinporousmedia, 1972.

[11] J. Poonoosamy, C. Soulaine, A. Burmeister, G. Deissmann, D. Bosbach, S. Roman, Microfluidic flow-through reactor and 3D Raman imaging for in situ assessment of mineral reactivity in porous and fractured porous media, Lab-on-a-Chip 20 (14) (2020) 2562–2571, doi:10.1039/d0lc00360c.

[12] N. Seigneur, K. U. Mayer, C. I. Steefel, Reactive Transport in Evolving Porous Media, Reviews in Mineralogy and Geochemistry 85 (1) (2019) 197–238, doi:10.2138/rmg.2019.85.7.

[13] M. Xie, K. U. Mayer, F. Claret, P. Alt-Epping, D. Jacques, C. Steefel, C. Chiaberge, J. Simunek, Implementation and evaluation of permeability-porosity and tortuosity-porosity relationships linked to mineral dissolution-precipitation, Computational geosciences 19 (3) (2015) 655–671.

[14] G. Daccord, R. Lenormand, Fractal patterns from chemical dissolution, Nature 325 (6099) (1987) 41–43.

[15] C. Garing, P. Gouze, M. Kassab, M. Riva, A. Guadagnini, Anti-correlated Porosity–Permeability Changes During the Dissolution of Carbonate Rocks: Experimental Evidences and Modeling, Transport in Porous Media 107 (2) (2015) 595–621.

[16] S. Bkri, J.-F. Thovert, P. Adler, Dissolution and deposition in fractures, Engineering Geology 48 (3-4) (1997) 283–308, doi:10.1016/S0013-7952(97)00044-6.

[17] L. Chen, Q. Kang, B. A. Robinson, Y.-L. He, W.-Q. Tao, Pore-scale modeling of multiphase reactive transport with phase transitions and dissolution-precipitation processes in closed systems, Phys. Rev. E 87 (2013) 043306, doi:10.1103/PhysRevE.87.043306, URL http://link.aps.org/doi/10.1103/PhysRevE.87.043306.

[18] A. M. Tartakovsky, P. Meakin, T. D. Scheibe, R. M. E. West, Simulations of reactive transport and precipitation with smoothed particle hydrodynamics, Journal of Computational Physics 222 (2) (2007) 654–672.

[19] S. Molins, D. Trebotich, L. Yang, J. B. Ajo-Franklin, T. J. Ligocki, C. Shen, C. I. Steefel, Pore-scale controls on calcite dissolution rates from flow-through laboratory and numerical experiments, Environmental science & technology 48 (13) (2014) 7453–7460.

[20] S. Molins, D. Trebotich, G. H. Miller, C. I. Steefel, Mineralogical and transport controls on the evolution of porous media texture using direct numerical simulation, Water Resources Research 53 (5) (2017) 3645–3661.

[21] S. Whitaker, The Method of Volume Averaging, vol. 13 of *Theory and Applications of Transport in Porous Media*, Dorderecht: Kluwer Academic, 1999.

[22] C. Soulaine, Y. Davit, M. Quintard, A two-pressure model for slightly compressible single phase flow in bi-structured porous media, Chemical Engineering Science

96 (0) (2013) 55 – 70, ISSN 0009-2509, doi:10.1016/j.ces.2013.03.060, URL http://www.sciencedirect.com/science/article/pii/S0009250913002492.

[23] M. J. Blunt, B. Bijeljic, H. Dong, O. Gharbi, S. Iglauer, P. Mostaghimi, A. Paluszny, C. Pentland, Pore-scale imaging and modelling, Advances in Water Resources 51 (2013) 197–216.

[24] H. Andr, N. Combaret, J. Dvorkin, E. Glatt, J. Han, M. Kabel, Y. Keehm, F. Krzikalla, M. Lee, C. Madonna, M. Marsh, T. Mukerji, E. H. Saenger, R. Sain, N. Saxena, S. Ricker, A. Wiegmann, X. Zhan, Digital rock physics benchmarks Part I: Imaging and segmentation, Computers & Geosciences 50 (0) (2013) 25 – 32, ISSN 0098-3004, doi:http://dx.doi.org/10.1016/j.cageo.2012.09.005, URL http://www.sciencedirect.com/science/article/pii/S0098300412003147, benchmark problems, datasets and methodologies for the computational geosciences.

[25] H. Andr, N. Combaret, J. Dvorkin, E. Glatt, J. Han, M. Kabel, Y. Keehm, F. Krzikalla, M. Lee, C. Madonna, M. Marsh, T. Mukerji, E. H. Saenger, R. Sain, N. Saxena, S. Ricker, A. Wiegmann, X. Zhan, Digital rock physics benchmarks Part II: Computing effective properties, Computers & Geosciences 50 (0) (2013) 33 – 43, ISSN 0098-3004, doi:http://dx.doi.org/10.1016/j.cageo.2012.09.008, URL http://www.sciencedirect.com/science/article/pii/S0098300412003172, benchmark problems, datasets and methodologies for the computational geosciences.

[26] C. Soulaine, J. Maes, S. Roman, Computational Microfluidics for Geosciences, Frontiers in Water 3 (2021) 1–11, doi:10.3389/frwa.2021.643714.

[27] P. Spanne, J. Thovert, C. Jacquin, W. Lindquist, K. Jones, P. Adler, Synchrotron computed microtomography of porous media: topology and transports, Physical Review Letters 73 (14) (1994) 2001.

[28] B. Bijeljic, A. Raeini, P. Mostaghimi, M. J. Blunt, Predictions of non-Fickian solute transport in different classes of porous media using direct simulation on pore-scale images, Phys. Rev. E 87 (2013) 013011, doi:10.1103/PhysRevE.87.013011, URL http://link.aps.org/doi/10.1103/PhysRevE.87.013011.

[29] R. Guibert, M. Nazarova, P. Horgue, G. Hamon, P. Creux, G. Debenest, Computational permeability determination from pore-scale imaging: Sample size, mesh and method sensitivities, Transport in Porous Media 107 (3) (2015) 641–656, ISSN 0169-3913, doi:10.1007/s11242-015-0458-0.

[30] C. Soulaine, F. Gjetvaj, C. Garing, S. Roman, A. Russian, P. Gouze, H. Tchelepi, The impact of sub-resolution porosity of X-ray microtomography images on the permeability, Transport in Porous Media 113 (1) (2016) 227–243, doi:10.1007/s11242-016-0690-2.

[31] P. Horgue, F. Augier, P. Duru, M. Prat, M. Quintard, Experimental and numerical study of two-phase flows in arrays of cylinders, Chemical Engineering Science 102 (0) (2013)

335 – 345, ISSN 0009-2509, doi:http://dx.doi.org/10.1016/j.ces.2013.08.031, URL http://www.sciencedirect.com/science/article/pii/S0009250913005745.

[32] A. Q. Raeini, M. J. Blunt, B. Bijeljic, Direct simulations of two-phase flow on micro-CT images of porous media and upscaling of pore-scale forces, Advances in Water Resources 74 (0) (2014) 116–126, ISSN 0309-1708, URL http://www.sciencedirect.com/science/article/pii/S0309170814001730.

[33] M. Graveleau, C. Soulaine, H. A. Tchelepi, Pore-Scale Simulation of Interphase Multicomponent Mass Transfer for Subsurface Flow, Transport in Porous Media 120 (2) (2017) 287–308.

[34] J. Maes, C. Soulaine, A new compressive scheme to simulate species transfer across fluid interfaces using the Volume-Of-Fluid method, Chemical Engineering Science 190 (2018) 405–418.

[35] S. Pavuluri, J. Maes, J. Yang, M. Regaieg, A. Moncorg, F. Doster, Towards pore network modelling of spontaneous imbibition: contact angle dependent invasion patterns and the occurrence of dynamic capillary barriers, Computational Geosciences 24 (2020) 951–969, doi:10.1007/s10596-019-09842-7.

[36] C. Noiriel, C. Soulaine, Pore-scale imaging and modelling of reactive flow in evolving porous media: tracking the dynamics of the fluid-rock interface, Transport in Porous Media doi:10.1007/s11242-021-01613-2.

[37] S. Molins, C. Soulaine, N. Prasianakis, A. Abbasi, P. Poncet, A. Ladd, V. Starchenko, S. Roman, D. Trebotich, H. Tchelepi, C. Steefel, Simulation of mineral dissolution at the pore scale with evolving fluid-solid interfaces: Review of approaches and benchmark problem set, Computational Geosciences (2020) 1–34ISSN 1573–1499.

[38] C. Soulaine, S. Roman, A. Kovscek, H. A. Tchelepi, Mineral dissolution and wormholing from a pore-scale perspective, Journal of Fluid Mechanics 827 (2017) 457–483, doi:10.1017/jfm.2017.499.

[39] F. Dutka, V. Starchenko, F. Osselin, S. Magni, P. Szymczak, A. J. Ladd, Time-dependent shapes of a dissolving mineral grain: Comparisons of simulations with microfluidic experiments, Chemical Geology 540 (2020) 119459.

[40] X. Liu, P. Ortoleva, A general-purpose, geochemical reservoir simulator, in: SPE Annual Technical Conference and Exhibition, Society of Petroleum Engineers, 1996.

[41] X. Liu, A. Ormond, K. Bartko, L. Ying, P. Ortoleva, A geochemical reaction-transport simulator for matrix acidizing analysis and design, Journal of Petroleum Science and Engineering 17 (1) (1997) 181–196.

[42] S. Molins, D. Trebotich, B. Arora, C. I. Steefel, H. Deng, Multi-scale model of reactive transport in fractured media: diffusion limitations on rates, Transport in Porous Media 128 (2) (2019) 701–721.

[43] G. S. Beavers, D. D. Joseph, Boundary conditions at a naturally permeable wall, Journal of Fluid Mechanics 30 (1967) 197–207, doi:10.1017/S0022112067001375.

[44] J. A. Ochoa-Tapia, S. Whitaker, Momentum transfer at the boundary between a porous medium and a homogeneous fluid: I. Theoretical development, International Journal of Heat and Mass Transfer 38 (14) (1995) 2635–2646.

[45] C. I. Steefel, L. E. Beckingham, G. Landrot, Micro-continuum approaches for modeling pore-scale geochemical processes, Rev Mineral Geochem 80 (2015) 217–246, doi:10.2138/rmg.2015.80.07.

[46] C. Soulaine, H. A. Tchelepi, Micro-continuum approach for pore-scale simulation of subsurface processes, Transport In Porous Media 113 (2016) 431–456, doi:10.1007/s11242-016-0701-3.

[47] A. Ormond, P. Ortoleva, Numerical modeling of reaction-induced cavities in a porous rock, Journal of Geophysical Research: Solid Earth 105 (B7) (2000) 16737–16747.

[48] F. Golfier, C. Zarcone, B. Bazin, R. Lenormand, D. Lasseux, M. Quintard, On the ability of a Darcy-scale model to capture wormhole formation during the dissolution of a porous medium, Journal of fluid Mechanics 457 (2002) 213–254.

[49] C. Arns, F. Bauget, A. Limaye, A. Sakellariou, T. Senden, A. Sheppard, R. Sok, W. Pinczewski, S. Bakke, L. Berge, P.-E. Oeren, M. Knackstedt, Pore-Scale Characterization of Carbonates Using X-Ray Microtomography, SPE Journal 10 (4) (2005) 475–484.

[50] S. N. Apourvari, C. H. Arns, An Assessment of the Influence of Micro-porosity for Effective Permeability Using Local Flux Analysis on Tomographic Images, International Petroleum Technology Conference, 19-22 January, Doha, Qatar .

[51] T. D. Scheibe, W. A. Perkins, M. C. Richmond, M. I. McKinley, P. D. J. Romero-Gomez, M. Oostrom, T. W. Wietsma, J. A. Serkowski, J. M. Zachara, Pore-scale and multiscale numerical simulation of flow and transport in a laboratory-scale column, Water Resources Research 51 (2) (2015) 1023–1035, ISSN 1944-7973, doi:10.1002/2014WR015959, URL http://dx.doi.org/10.1002/2014WR015959.

[52] C. Soulaine, P. Creux, H. A. Tchelepi, Micro-Continuum Framework for Pore-Scale Multiphase Fluid Transport in Shale Formations, Transport in Porous Media 127 (2019) 85–112.

[53] P. Horgue, C. Soulaine, J. Franc, R. Guibert, G. Debenest, An open-source toolbox for multiphase flow in porous media, Computer Physics Communications 187 (0) (2015) 217– 226, ISSN 0010-4655, doi:http://dx.doi.org/10.1016/j.cpc.2014.10.005, URL http://www.sciencedirect.com/science/article/pii/S0010465514003403.

[54] J. Maes, S. Geiger, Direct pore-scale reactive transport modelling of dynamic wettability changes induced by surface complexation, Advances in Water Resources 111 (2018) 6–19.

[55] L. Orgogozo, N. Renon, C. Soulaine, F. Hnon, S. Tomer, D. Labat, O. Pokrovsky, M. Sekhar, R. Ababou, M. Quintard, An open source massively parallel solver for Richards equation: Mechanistic modelling of water fluxes at the watershed scale, Computer Physics Communications 185 (12) (2014) 3358 – 3371, ISSN 0010-4655, doi:http://dx.doi.org/10.1016/j.cpc.2014.08.004, URL http://www.sciencedirect.com/science/article/pii/S0010465514002719.

[56] D. L. Parkhurst, L. Wissmeier, PhreeqcRM: A reaction module for transport simulators based on the geochemical model PHREEQC, Advances in Water Resources 83 (2015) 176–189.

[57] M. Rolle, R. Sprocati, M. Masi, B. Jin, M. Muniruzzaman, Nernst-Planck-based Description of Transport, Coulombic Interactions, and Geochemical Reactions in Porous Media: Modeling Approach and Benchmark Experiments, Water Resources Research 54 (4) (2018) 3176–3195, doi:https://doi.org/10.1002/2017WR022344, URL https://agupubs.onlinelibrary.wiley.com/doi/abs/10.1002/2017WR022344.

[58] R. W. Healy, S. S. Haile, D. L. Parkhurst, S. R. Charlton, VS2DRTI: Simulating Heat and Reactive Solute Transport in Variably Saturated Porous Media, Groundwater 56 (5) (2018) 810–815, doi:https://doi.org/10.1111/gwat.12640, URL https://ngwa.onlinelibrary.wiley.com/doi/abs/10.1111/gwat.12640.

[59] M. Muniruzzaman, M. Rolle, Multicomponent Ionic Transport Modeling in Physically and Electrostatically Heterogeneous Porous Media With PhreeqcRM Coupling for Geochemical Reactions, Water Resources Research 55 (12) (2019) 11121–11143, doi:https://doi.org/10.1029/2019WR026373, URL https://agupubs.onlinelibrary.wiley.com/doi/abs/10.1029/2019WR026373.

[60] M. Muniruzzaman, T. Karlsson, N. Ahmadi, M. Rolle, Multiphase and multicomponent simulation of acid mine drainage in unsaturated mine waste: Modeling approach, benchmarks and application examples, Applied Geochemistry 120 (2020) 104677, ISSN 0883-2927, doi:https://doi.org/10.1016/j.apgeochem.2020.104677, URL https://www.sciencedirect.com/science/article/pii/S0883292720301682.

[61] J. Moortgat, M. Li, M. Amooie, D. Zhu, A higher-order finite element reactive transport model for unstructured and fractured grids, Scientific Reports 10 (2020) 15572, doi:https://doi.org/10.1038/s41598-020-72354-3.

[62] H. C. Brinkman, A Calculation of The Viscous Force Exerted by a Flowing Fluid on a Dense Swarm of Particles, Appl. Sci. Res. A1 (1947) 27–34.

[63] G. Neale, W. Nader, Practical significance of Brinkman's extension of Darcy's law: coupled parallel flows within a channel and a bounding porous medium, The Canadian Journal of Chemical Engineering 52 (4) (1974) 475–478.

[64] K. Vafai, C. Tien, Boundary and inertia effects on flow and heat transfer in porous media, International Journal of Heat and Mass Transfer 24 (2) (1981) 195–203.

[65] C. Hsu, P. Cheng, Thermal dispersion in a porous medium, International Journal of Heat and Mass Transfer 33 (8) (1990) 1587–1597.

[66] P. Bousquet-Melou, B. Goyeau, M. Quintard, F. Fichot, D. Gobin, Average momentum equation for interdendritic flow in a solidifying columnar mushy zone, International Journal of Heat and Mass Transfer 45 (17) (2002) 3651 – 3665, ISSN 0017-9310, doi: http://dx.doi.org/10.1016/S0017-9310(02)00077-7, URL http://www.sciencedirect.com/science/article/pii/S0017931002000777.

[67] B. Goyeau, D. Lhuillier, D. Gobin, M. Velarde, Momentum transport at a fluid–porous interface, International Journal of Heat and Mass Transfer 46 (21) (2003) 4071–4081.

[68] P. Angot, C.-H. Bruneau, P. Fabrie, A penalization method to take into account obstacles in incompressible viscous flows, Numerische Mathematik 81 (4) (1999) 497–520.

[69] F. J. Carrillo, I. C. Bourg, A Darcy-Brinkman-Biot Approach to Modeling the Hydrology and Mechanics of Porous Media Containing Macropores and Deformable Microporous Regions, Water Resources Research 55 (10) (2019) 8096–8121, doi:10.1029/2019WR024712, URL https://agupubs.onlinelibrary.wiley.com/doi/abs/10.1029/2019WR024712.

[70] N. Seigneur, V. Lagneau, J. Corvisier, A. Dauzres, Recoupling flow and chemistry in variably saturated reactive transport modelling - An algorithm to accurately couple the feedback of chemistry on water consumption, variable porosity and flow, Advances in Water Resources 122 (2018) 355–366, ISSN 0309-1708, doi:https://doi.org/10.1016/j.advwatres.2018.10.025, URL https://www.sciencedirect.com/science/article/pii/S0309170818306304.

[71] R. I. Issa, Solution of the Implicitly Discretised Fluid Flow Equations by Operator-Splitting, Journal of Computational Physics 62 (1985) 40–65.

[72] S. V. Patankar, Numerical Heat Transfer And Fluid Flow, Taylor & Francis, Washington, DC, 1980.

[73] D. Parkhurst, C. Appelo, Description of input and examples for PHREEQC Version 3a computer program for speciation, batch-reaction, one-dimensional transport, and

inverse geochemical calculations, vol. 6-A43, U.S. Department of the Interior, U.S. Geological Survey Techniques and Methods, 2013.

[74] G. Strang, On the Construction and Comparison of Difference Schemes, SIAM Journal on Numerical Analysis 5 (3) (1968) pp. 506–517, ISSN 00361429, URL http://www.jstor.org/stable/2949700.

[75] J. Kozeny, Uber kapillare leitung der wasser in boden, Royal Academy of Science, Vienna, Proc. Class I 136 (1927) 271–306.

[76] P. C. Carman, Fluid flow through granular beds, Trans. Inst. Chem. Eng. 15 (1937) 150–166.

[77] A. Verma, K. Pruess, Thermohydrological conditions and silica redistribution near high-level nuclear wastes emplaced in saturated geological formations, Journal of Geophysical Research: Solid Earth 93 (B2) (1988) 1159–1173, doi:10.1029/JB093iB02p01159, URL https://agupubs.onlinelibrary.wiley.com/doi/abs/10.1029/JB093iB02p01159.

[78] S. Roman, C. Soulaine, M. A. AlSaud, A. Kovscek, H. Tchelepi, Particle velocimetry analysis of immiscible two-phase flow in micromodels, Advances in Water Resources 95 (2016) 199–211, ISSN 0309-1708, doi:http://dx.doi.org/10.1016/j.advwatres.2015.08.015, URL http://www.sciencedirect.com/science/article/pii/S0309170815002018.

[79] C. Noiriel, L. Luquot, B. Mad, L. Raimbault, P. Gouze, J. van der Lee, Changes in reactive surface area during limestone dissolution: An experimental and modelling study, Chemical Geology 265 (12) (2009) 160 – 170, ISSN 0009-2541, doi:http://dx.doi.org/10.1016/j.chemgeo.2009.01.032, URL http://www.sciencedirect.com/science/article/pii/S0009254109000643, cO2 geological storage: Integrating geochemical, hydrodynamical, mechanical and biological processes from the pore to the reservoir scale.

[80] N. I. Prasianakis, M. Gatschet, A. Abbasi, S. V. Churakov, Upscaling Strategies of Porosity-Permeability Correlations in Reacting Environments from Pore-Scale Simulations, Geofluids 2018 (2018) 1–8, ISSN 1468-8115, doi:10.1155/2018/9260603.

[81] V. Starchenko, C. J. Marra, A. J. Ladd, Three-dimensional simulations of fracture dissolution, Journal of Geophysical Research: Solid Earth 121 (2016) 6421–6444, doi:10.1002/2016JB013321.

[82] D. Sanchez, L. Hume, R. Chatelin, P. Poncet, Analysis of the 3D non-linear Stokes problem coupled to transport-diffusion for shear-thinning heterogeneous microscale flows, applications to digital rock physics and mucociliary clearance, Math. Model.Numer. Anal. 53 (2019) 1083–1124, ISSN 0764-583X, doi:10.1051/m2an/2019013.

[83] C. Noiriel, B. Madé, P. Gouze, Impact of coating development on the hydraulic and transport properties in argillaceous limestone fracture, Water resources research 43 (9) (2007) 1–16.

[84] J. Ajo-Franklin, M. Voltolini, S. Molins, L. Yang, Coupled Processes in a Fractured Reactive System: A Dolomite Dissolution Study with Relevance to GCS Caprock Integrity., in: Caprock Integrity in Geological Storage: Hydrogeochemical and Hydrogeomechanical Processes and their Impact on Storage Security, Wiley Publishing: New York, 2018.

[85] J. Poonoosamy, C. Wanner, P. Alt Epping, J. F. guila, J. Samper, L. Montenegro, M. Xie, D. Su, K. U. Mayer, U. Mder, L. R. Van Loon, G. Kosakowski, Benchmarking of reactive transport codes for 2D simulations with mineral dissolutionprecipitation reactions and feedback on transport parameters, Computational Geosciences (2018) 1–22doi:10.1007/s10596-018-9793-x.

[86] H. Deng, J. P. Fitts, R. V. Tappero, J. J. Kim, C. A. Peters, Acid Erosion of Carbonate Fractures and Accessibility of Arsenic-Bearing Minerals: In Operando Synchrotron-Based Microfluidic Experiment, Environmental Science & Technology 54 (19) (2020) 12502–12510, doi:10.1021/acs.est.0c03736, URL https://doi.org/10.1021/acs.est.0c03736, pMID: 32845141.

[87] A. Nissan, U. Alcolombri, F. de Schaetzen, B. Berkowitz, J. Jimenez-Martinez, Reactive Transport with FluidSolid Interactions in Dual-Porosity Media, ACS EST Water ISSN 2690-0637, doi:10.1021/acsestwater.0c00043.

[88] F. Osselin, P. Kondratiuk, A. Budek, O. Cybulski, P. Garstecki, P. Szymczak, Microfluidic observation of the onset of reactive-infitration instability in an analog fracture, Geophysical Research Letters 43 (2016) 6907–6915, ISSN 0094-8276, doi:10.1002/2016gl069261.

[89] C. Soulaine, S. Roman, A. Kovscek, H. A. Tchelepi, Pore-scale modelling of multiphase reactive flow. Application to mineral dissolution with production of CO2, Journal of Fluid Mechanics 855 (2018) 616645, doi:10.1017/jfm.2018.655.

[90] F. J. Carrillo, I. C. Bourg, C. Soulaine, Multiphase flow modeling in multiscale porous media: An open-source micro-continuum approach, Journal of Computational Physics: X 8 (2020) 100073, ISSN 2590-0552, doi:10.1016/j.jcpx.2020.100073.

Dear Editor,

We declare no conflict of interest.

Best regards,

Cyprien Soulaine
(cyprien.soulaine@cnrs-orleans.fr)

Highlights

- We developped an open-source platform for multi-scale simulations of hydro-geochemical processes,
- A unique formulation can handle pore-scale, hybrid-scale and continuum-scale simulations for hydro-geochemical processes,
- The framework is verified using reference solutions both at the pore-scale and at continuum-scale using PHREEQC,
- We investigate reactive transport in a fractured porous medium at the hybrid-scale.

Declaration of interests

■ The authors declare that they have no known competing financial interests or personal relationships that could have appeared to influence the work reported in this paper.

☐The authors declare the following financial interests/personal relationships which may be considered as potential competing interests: